Original research article

First-principles study of the structural, electronic and optical properties of MgF$_2$

A. Arroussi [a], M. Ghezali [a],[b],[*]

[a] *Laboratoire de Microphysique et de Nanophysique (LaMiN), ENP-Oran, BP 1523 El M'Naouer, Oran 31000, Algeria*
[b] *Département des Sciences de la Matière, Faculté des Sciences Exactes, Université Tahri Mohamed Béchar, BP 417 Rue de Kanadissa, 08000 Bechar, Algeria*

A B S T R A C T

MgF$_2$ is a compound, which is transparent for the entire spectrum ranging from ultraviolet to infrared is a good candidate for ultraviolet applications. In this work, we have studied the structural, electronic and optical properties of MgF$_2$ by the first principles method of FP-LMTO method based on the density functional theory DFT in three phases in which our material is likely to crystallize. We also verified the phase transitions. The most remarkable is the similarity between the properties of the three phases at all levels (gaps, optical constants, ionicity). The comparison between our results and the literature has shown satisfactory agreement.

© 2018 Elsevier GmbH. All rights reserved.

1. Introduction

MgF$_2$ is a transparent material for the entire spectrum ranging from ultraviolet to infrared and is a good candidate especially for ultraviolet applications. This fact explains the abundance of work that is currently dedicated to it, but another reason lies in the fact that this material has structural properties related to defects and pressure that make it a subject of academic study very interesting. This material is used in various applications such as anti-reflective coatings and for polarization of light [1,2]. It is also within the concept of different optical devices such as prisms, lenses, telescopes, cameras, etc. It turns out to be a new optical material for semiconductor lithography because of its transmission characteristic in the ultraviolet region under vacuum [3]. Many other applications are possible paramount importance such as solar cells, ultraviolet lasers, organic light emitting diodes (organic LEDs) [4,5] etc.

MgF$_2$ is a solid material, resistant to chemical attack, laser deterioration and mechanical and thermal shock. MgF$_2$ is a rugged material resistant to chemical etching, laser damage, and mechanical and thermal shock. It has a Knoop Hardness of 415 and index of refraction of 1.38. The magnesium fluoride is a positive birefringent crystal obtained under vacuum by the Stockbarger method [6]. It is generally oriented with its c-axis parallel to the optical axis to minimize the birefringent effects. Under normal working conditions, polished surfaces of magnesium fluoride do not degrade. For temperatures above 500 °C, they degrade in the presence of moisture. Magnesium fluoride is inert to organic chemicals and many acids, including HF acid. It dissolves slowly in nitric acid. Note that in a dry environment, magnesium fluoride can be used up to 800 °C [10]. The MgF$_2$ is considered a good candidate for ultraviolet use and is transparent for the spectrum from ultraviolet to infrared.

---

* Corresponding author at: Département des Sciences de la Matière, Faculté des Sciences Exactes, Université Tahri Mohamed Béchar, BP 417 Rue de Kanadissa, 08000 Béchar, Algéria.
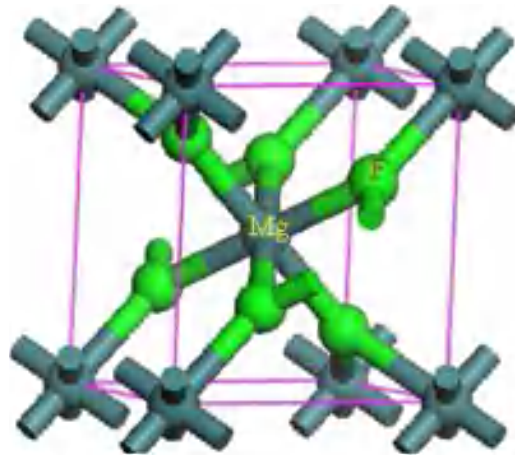*E-mail address:* ghazali.mohammed@univ-bechar.dz (M. Ghezali).
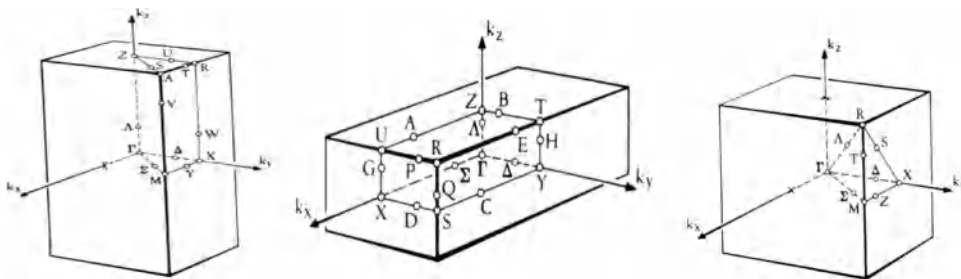
Fig. 1. The crystalline form of MgF$_2$ [14].

Fig. 2. The Brillouin zone and the high symmetry points of tetragonal, orthorhombic and cubic phase [18].

TECHSPEC® magnesium fluoride windows provide excellent broadband transmission from the ultraviolet to mid-infrared range. It is used in many technological applications, including electrolysis, glasses manufacturing, prisms and anti-reflective coatings [11,12].

The MgF$_2$ compound crystallizes as tetragonal birefringent crystals. Its structure is analogous to that of rutile (TiO$_2$), with centers of Mg^{2+} octahedral and three coordinates of fluoride centers [13]. The crystalline form of this compound (Fig. 1) is tetragonal where the parameters of mesh $a = b \neq c$. It is the same known structure in TiO$_2$ (rutile), where the node is composed of two Mg atoms located in the coordinates *(0,0,0)* and *(1/2,1/2,1/2),* and four F atoms located in *(x, x, 0), (-x, -x, 0), (1/2 + x, 1/2-x, 1/2)* and *(1 / 2- x, 1/2 +x, 1/2)* where x is an internal parameter. Thus, the reciprocal lattice of our simple tetragonal, orthorhombic and cubic is presented in Fig. 2. The high symmetry points used in our calculations are also shown in this figure.

The MgF$_2$ compound is a semiconductor in direct bandgap, the minimum of the conduction band (CB) and the maximum of the valence band (VB) are located at the point Γ of the Brillouin zone. This allows direct transitions between VB and CB [17]. MgF$_2$ has a direct optical transition with a direct band gap of 10.8 eV [15]. Magnesium fluoride is therefore a broad bandgap and therefore, it is used in the far ultraviolet.

2. Methods

The calculations presented in this work were carried out using the full potential linear muffin-tin orbital method (FPLMTO) in which the non-overlapping muffin tin spheres potential is Fourier transformed in the interstitial regions and hence treats the interstitial regions on the same footing with the core regions [7]. The exchange correlation energy of electrons is described in both the local density approximation (LDA) [8,9] using the parameterisation of Perdew et al. [10,11]. FPLMTO have been carried out using the Lmtart [7,12] code.

In FPLMTO, the non-overlapping muffin tin spheres MTS potential is expanded in spherical harmonics inside the spheres of radius RMTS. In the interstitial region, the *s, p* and *d* basis functions are expanded in a number (NPLW) of plane waves determined automatically by the cut-off energies. The details of calculations are as follows: the charge density and the potential are represented inside the muffin-tin (MT) spheres by spherical harmonics up to lmax = 6. The self-consistent calculations are considered to be converged when total energy of the system in stable within 10^{-4} Ry (Table 1).

Table 1

Parameters used in the FPLMTO calculations for different phases: NPLW is the number of plane waves used in the interstitial regions, E_{cut} is the cut-off energy in Rydbergs, RMTS is in atomic units and K-point represents the number of special K-points in the irreducible BZ involved in the calculations.

Parameters	Rutile TiO$_2$	CaCl$_2$	Modified Fluoride PdF$_2$
l_{max}	6	6	6
Total NPLW	21162	20386	44472
RMTS (Mg)	2.054	2.054	2.078
RMTS (F)	1.681	2.065	1.700
E_{cut}	203.1919	202.2732	223.2928
K-point	(44,44,28)	(42,42,28)	(46,46,46)
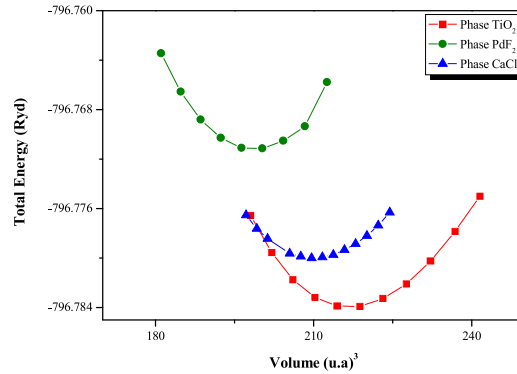
Fig. 3. Total energy versus volume for the three phases.

3. Results and discussion

3.1. Structural properties

We have studied our material in different susceptible structures in which MgF$_2$ is likely to crystallize as a function of applied pressure. Indeed, materials crystallize in different phases and have the ability to transform from one phase to another under the effect of temperature or pressure. The calculation of the total energy allows us to have the static equilibrium properties, which are represented by the network parameters a_0 (b_0 and c_0 if necessary), the internal parameters, the compressibility modulus B and its first derivative B'. To obtain these parameters, the curve of the total energy as a function of the volume is adjusted to the Murnaghan's equation of state [19] given by the following expression:

$$E(V) = E_0 + \left[\frac{BV}{B'(B'-1)} \right] \cdot \left[B' \left(1 - \frac{V_0}{V} \right) + \left(\frac{V_0}{V} \right)^{B'} - 1 \right] \tag{1}$$

In the preceding equation, the parameter V means the volume of the mesh at a given energy E, V_0 is the equilibrium volume corresponding to that of the ground state. E_0 represents the minimum energy corresponding to the volume of the equilibrium V_0, B_0 is the bulk modulus and B' is derived from the bulk modulus. The bulk modulus is deduced by:

$$B = V \frac{\partial^2 E}{\partial V^2} \tag{2}$$

Volume optimization was performed by minimizing the total energy (Fig. 3) with respect to the unit cell volume using Murnaghan's equation of state. The equilibrium lattice constant, the bulk modulus B and its derivative have been calculated. The results are summarized in Table 2.

In Table 3, the calculated pressures for which MgF$_2$ is expected to change phase have been listed and compared to the literature. For the transition to the CaCl$_2$ structure, the concordance is perfect. For the transition to the modified PdF$_2$ fluoride structure, we have good agreement for the CaCl$_2$ intermediate transition → PdF$_2$ (modified fluoride). We did not find any values for Rutile transition → PdF$_2$ (modified fluoride).

3.2. Electronic properties

Based on the LDA approximation of Perdew et al. [24], we calculated the band structure of the MgF$_2$ compound for the different phases studied above. The knowledge of the electronic structure is necessary to situate our material with respect to the applications.

Table 2
Calculated structural parameters of MgF$_2$, the bulk modulus B and its pressure derivative B' with x, y, z and u are the internal parameters.

Structure	Rutile TiO$_2$	CaCl$_2$	Modified Fluoride PdF$_2$
V_0 (au^3)	216.77[1]	209.99[1]	197.89[1]
V_0 (Å^3)	32.09[1]	31.09[1]	29.29[1]
a_0 (Å)	4.5998[1] 4.6028[a]	4.5763[1] 4.5920[e]	4.8935[1] 4.702[b]
	4.579[e] 4.621[j]	4.539[e] 4.516[i]	4.890[e] 4.762[i]
b_0/a_0		0.977[1] 1.05[c]	
		1.018[e] 0.9912[i]	
c_0/a_0	0.659[1] 0.6598[a]	0.664[1] 0.6691[e]	
	0.6599[b] 0.6599[i]	0.6399[b] 0.6608[i]	
x	0.305[1] 0.3026[a] 0.3034[c] 0.3029[j]	0.256[1] 0.306[i]	0.342[1] 0.3451[e] 0.3451[i]
y		0.359[1] 0.294[i]	
B_0 (GPa)	113.86[1] 111.47[a]	119.01[1] 105.4[e]	140.49[1] 133.8[e]
	117[d] 101 ± 3[i]	134[b]	114[f] 123 ± 3[i]
B_0'	4.56[1] 4.13[d]	3.31[1] 3.65[e]	3.62[1] 3.5[f]
	3.7[f] 4.2 ± 1.1[i]	3.7[f]	4[i]

[1] Our calculation.
[a] Ref. [14].
[b] Ref. [17].
[c] Ref. [20].
[d] Ref. [21].
[e] Ref. [22].
[f] Ref. [15].
[i] Ref. [15] expt.
[j] Ref. [16] expt.

Table 3
Transition pressure.

Transition	Pressure (Gpa)		
Rutile → CaCl$_2$	9.25[1]	9[a] 10[b] 12.3[c] 9.54[d] 9.0[e]	9.1[f]
Rutile → PdF$_2$	12.50[1]		
CaCl$_2$ → PdF$_2$	16.50[1]	14[c] 13.73[d] 13.5[e]	14[f]

[1] Our calculation.
[a] Ref. [21].
[b] Ref. [17].
[c] Ref. [15].
[d] Ref. [23].
[e] Ref. [20].
[f] Ref. [15] expt.
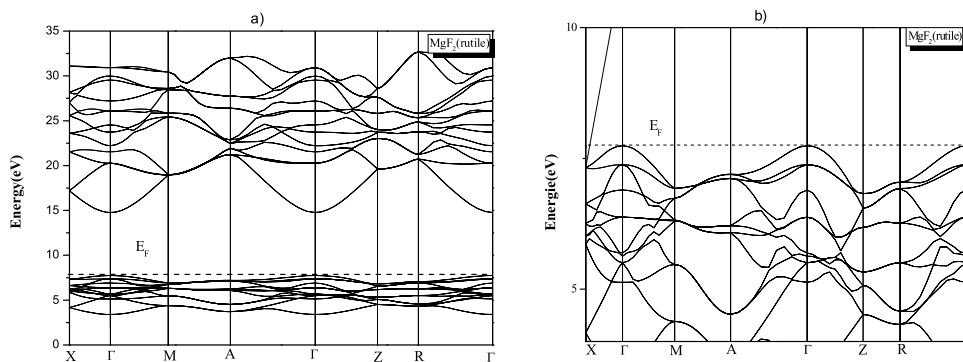
Fig. 4. MgF$_2$ band structure in rutile phase, b) Enlargement of the valence band.

The band structure of MgF$_2$ in the rutile phase is shown in Fig. 4a, it is noted that the maximum of the valence band (VB) is located at the point of high symmetry Γ, and the minimum of the conduction band (CB) is also at Γ. It is therefore a direct gap phase Eg = 7.024 eV, which is a wide gap. Babu et al. [14] find a direct gap with a value of Eg = 6.83 eV with the LDA without the scissors technique, and a value of Eg = 6.88 eV with GGA still without the scissors technique. Kanchana et al. [17] also find a direct gap with a value of Eg = 6.45 eV with the LDA combined with the TB-LMTO technique. The experimental value closest to our value gives a direct gap Eg (Γ-Γ) = 10.8 eV [9].

Table 4 presents other values taken from the literature to compare. Recall that the significant difference between calculated and measured gaps are a known artefact of the LDA theory.

Table 4
The MgF2 Gap for the three phases.

Structure	Rutile TiO$_2$	CaCl$_2$	Modified Fluoride PdF$_2$
Eg (eV)	7.024[1]	7.121[1]	7.165[1]
	6.83[a] 6.88[b] 6.45[c]	7.29[a]	7.10[a]
	9.5[d]		
	10.8[e] 13.0[f] 12.5[g]		

[1] Our calculation.
[a] Ref. [14] with LDA without the technique of ščissors.
[b] Ref. [14] with GGA without the technique of ščissors.
[c] Ref. [17] with LDA and TB-LMTO.
[d] Ref. [25] with la B3PW.
[e] Ref. [9].
[f] Ref. [27].
[g] Ref. [28].
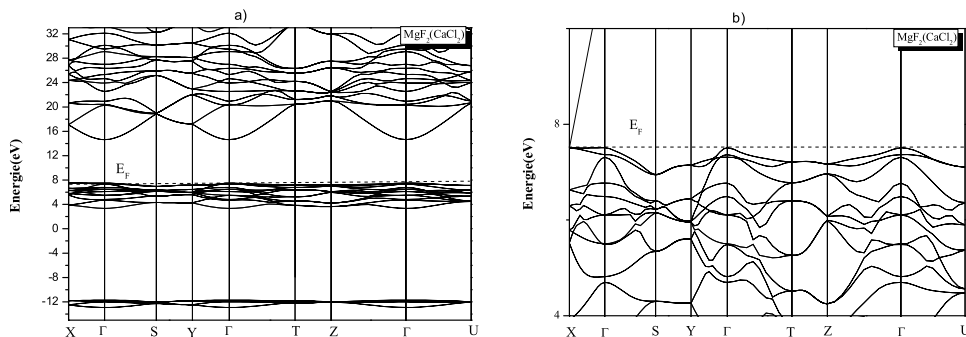
Fig. 5. MgF$_2$ band structure in CaCl$_2$ phase, b) Enlargement of the valence band.
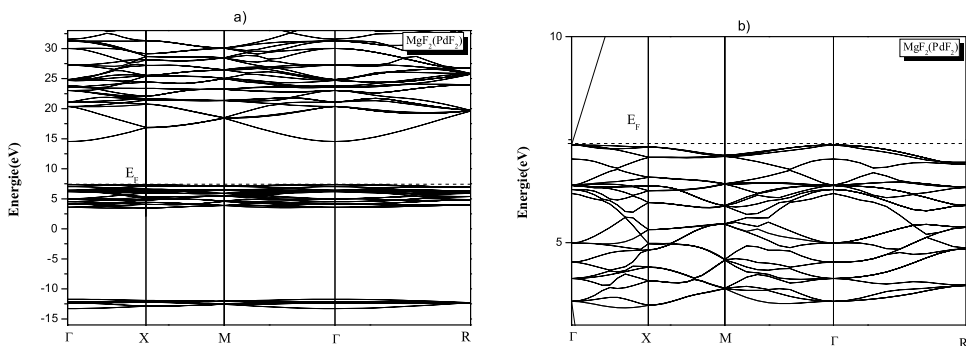
Fig. 6. MgF$_2$ band structure in PdF$_2$ phase, b) Enlargement of the valence band.

Finally, note the theoretical result of Abuova et al. [25] is very close to the experimental value, this being due to the use by the authors of B3PW method (Becke three parameters-functional flat-waves [26]). In Table 4, our results are listed with those of other authors.

In Fig. 5, it is indeed a phase with a direct gap Eg = 7.121 eV. Kanchana et al. [17] also find a direct gap with a value of Eg = 7.29 eV with LDA and TB-LMTO (Table 4).

From Fig. 6, we note that the maximum of the VB and the minimum of the CB are located at the point of high symmetry Γ. It is indeed a phase with a direct gap Eg = 7.165 eV. Kanchana et al. [17] also find a direct gap with Eg = 7.10 eV with LDA combined with TB-LMTO (Table 4).

What is remarkable is the fact that MgF$_2$ has the same direct gap in Γ in the 3 phases studied, and that the value of the latter remains about the same: 7.024 in rutile, 7.121 eV in CaCl$_2$ and 7.165 eV for the modified fluoride phase PdF$_2$.

The importance of the electronic properties of a material lies in the fact that they enable us to deduce the possible applications. Among these properties, the density of states in particular is directly related to macroscopic optical properties.

One of the objectives is to highlight the contribution of each atomic orbital to the density of state. This contribution is obviously attached to the electronic configuration. The individual contributions of the orbitals involved in this study are 3s-Mg, 3p-Mg, 3d-Mg, 2s-F and 2p-F (Figs. 7–9).
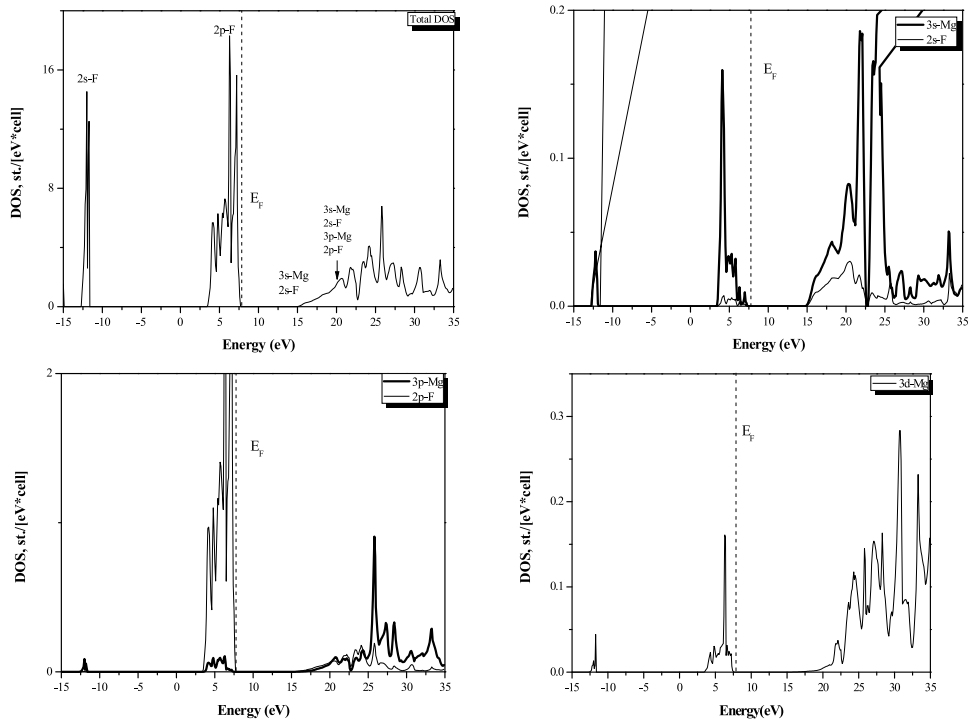
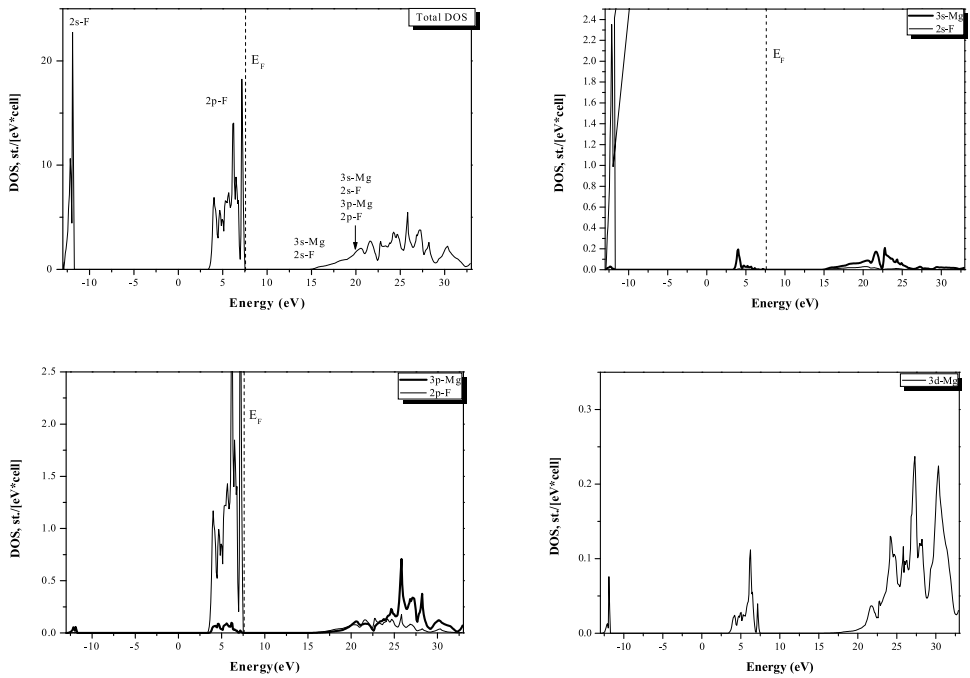**Fig. 7.** Total and Partial DOS of MgF$_2$ in Rutile Phase.

Fig. 8. Total and Partial DOS of MgF$_2$ in CaCl$_2$ Phase.
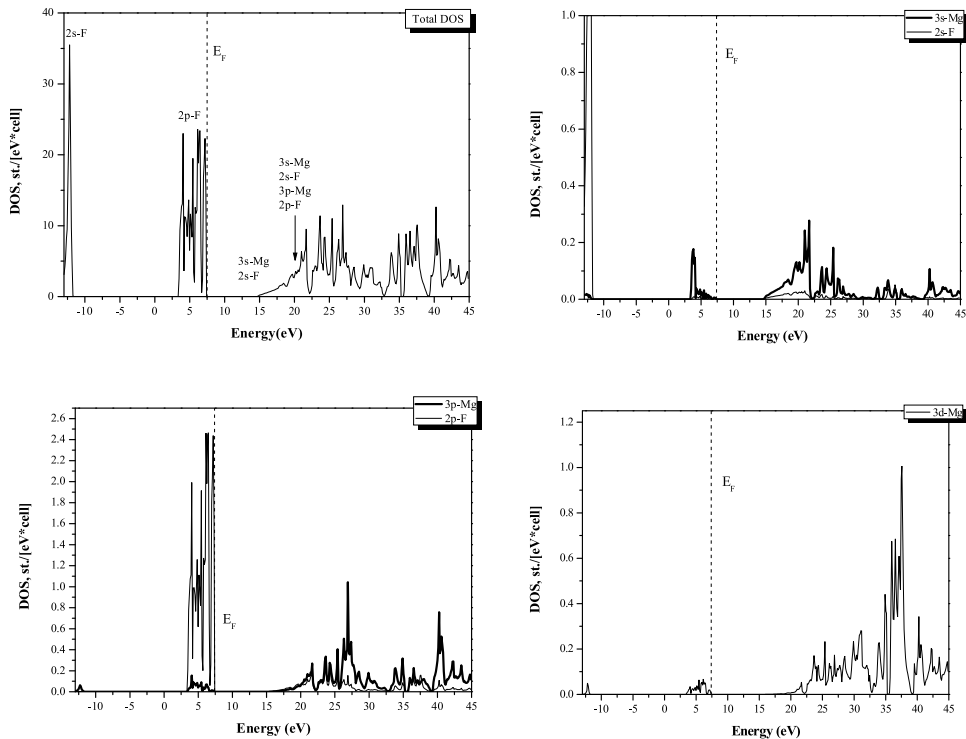
Fig. 9. Total and Partial DOS of MgF$_2$ in the modified fluoride phase PdF$_2$.

What is remarkable in this study is the almost perfect resemblance of the density of states in the three phases and this both in terms of the total DOS at the level of the contribution of each orbital taken apart. This similarity leads us to think that the optical properties of MgF$_2$ are not very sensitive to variations in pressure. For each of the three phases studied, the total density of states confirms the value of the gap obtained previously in the band structure calculation. An important remark is that the contribution of the 3d-Mg orbital seems to be negligible, which partly explains at least the large gap value because the orbitals d̈are known for their gap reduction effect.

In all cases, the VB is divided into two parts: the first part which is deep is dominated by the 2s states of the F atom (it ranges between −12.7 eV and −11.6 eV for rutile, −12.9 eV and −11.7 eV for CaCl$_2$, −13 eV and −11.7 eV for the modified fluoride phase PdF$_2$). The second part, located at the top of BV just before the gap is dominated by the 2p states of the F atom.

Just above the gap, at the beginning of the BC, and whatever the phase, it is the 3s and 2s orbitals of magnesium and fluorine respectively that dominate. Then follows an interval where the 3s-Mg, 2s-F, 3p-Mg and 2p-F orbitals contribute almost equally.

3.3. Optical properties

Recall that the real and imaginary parts of the dielectric function ε_1 and ε_2 can be obtained from each other by means of the Kramers-Kronig relation [29]. The imaginary dielectric constant $\varepsilon_2(\omega)$ depends on the dipole moment matrix, the initial and final states involved in the transitions, and the frequency ω of the absorbed or emitted photon.

In Fig.10, we represent the variation of the imaginary part of the dielectric function of MgF$_2$ in the rutile, CaCl$_2$ and modified fluoride PdF$_2$ phases as a function of energy. The inclusion of all phases in the same figure is justified by the fact that we want to compare their optical properties given the many similarities that have been found in the previous properties.

Fig. 11 shows the variation of the real part ε_1 of the dielectric function of MgF$_2$ in the rutile, CaCl$_2$ and modified fluoride PdF$_2$ phases as a function of energy. It appears from this figure that ε_1 is much more constant under the effect of pressure than ε_2. Indeed, the curves are virtually identical for the three phases.

It is clear now, by comparing the real and imaginary parts of the three phases, that these phases are expected to possess practically the same optical properties. This is confirmed by the calculation of three essential optical properties: the refractive index (Fig. 12), the absorption coefficient (Fig. 13) and the refraction coefficient (Fig. 14).

3.4. Charge density

The charge density is an important property in the solid, since it provides a good description of the chemical properties.
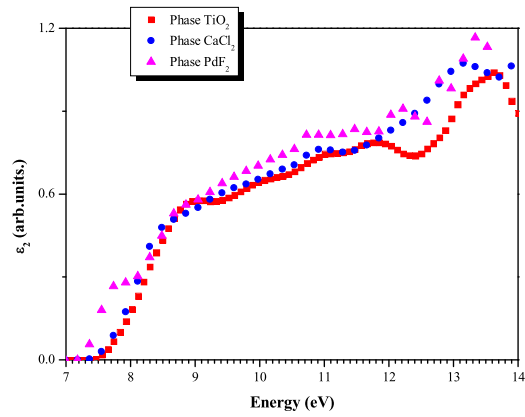
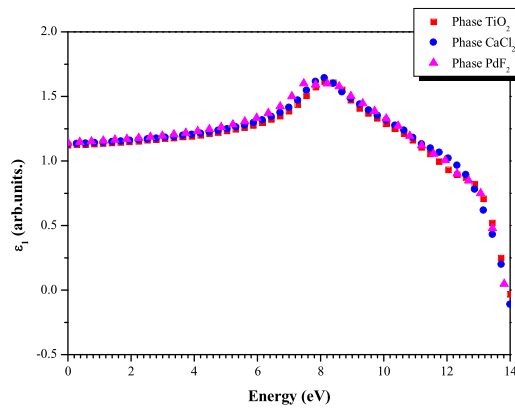**Fig. 10.** Imaginary part of the dielectric function of MgF_2.

Fig. 11. Real part of the dielectric function of MgF_2.
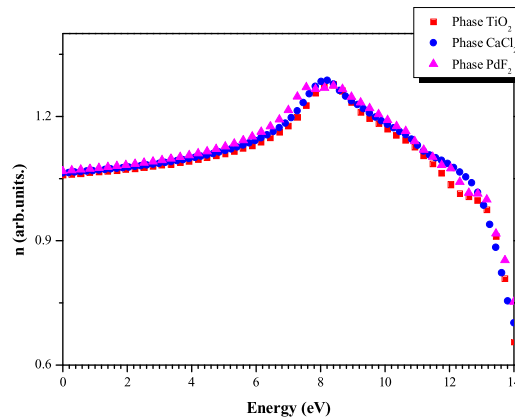

Fig. 12. Refractive index of MgF_2.

This density also makes it possible to study the crystalline structures and to predict their evolutions under the influence of an external disturbance. The ionic character is relative to the charge transfer between cations and anions. For this reason, we have calculated the loading densities of MgF2 in the rutile, $CaCl_2$ and modified fluoride PdF_2 phases.

The displacement of the charge increases as a function of the difference between the electronegativity values of two atoms.

Note in Fig.15 that the charge density vanishes almost over a long distance separating the two types of atoms (shown also in Fig. 16), suggesting a more ionic than a covalent bond.
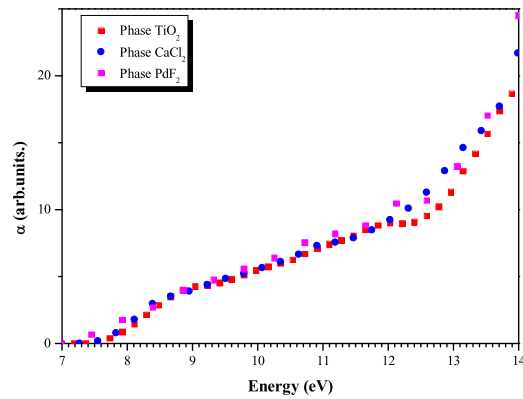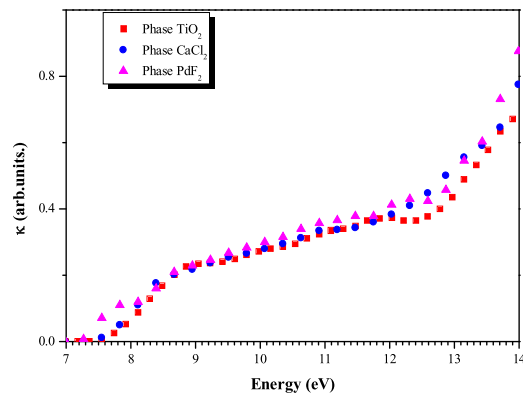
Fig. 13. Absorption coefficient of MgF$_2$.
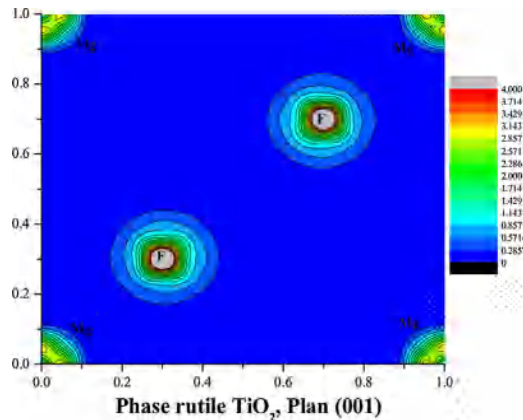

Fig. 14. Extinction coefficient of MgF$_2$.

Fig. 15. Charge density of the rutile phase of MgF$_2$ in the (001) plane.

The charge density in the (001) plane of the CaCl$_2$ structure of MgF$_2$ (Fig. 17) clearly shows a more ionic than a covalent character, which is in agreement with the reference [23] which finds that the covalent bond is weaker than the ionic bond. The arrangement of atoms is shown in Fig. 18.

The charge density in the same plane (001) of the PdF$_2$ structure of MgF$_2$ (Fig. 19) shows how it concentrates mainly near the atoms by becoming very small in the rest of the space. Fig. 19 does not show the link between nearest neighbours, so we have plotted Fig. 20 in the (110) plane which clearly shows a more ionic than a covalent character. The arrangement of atoms is shown in Fig. 21.
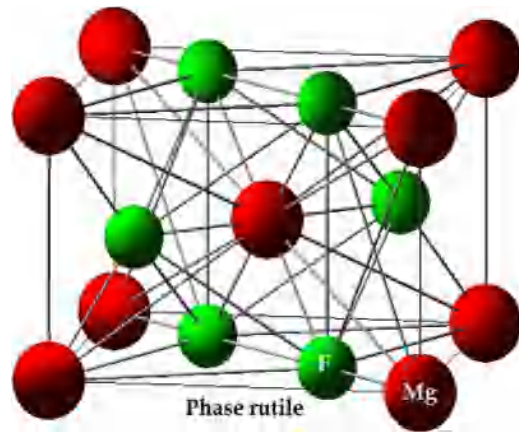
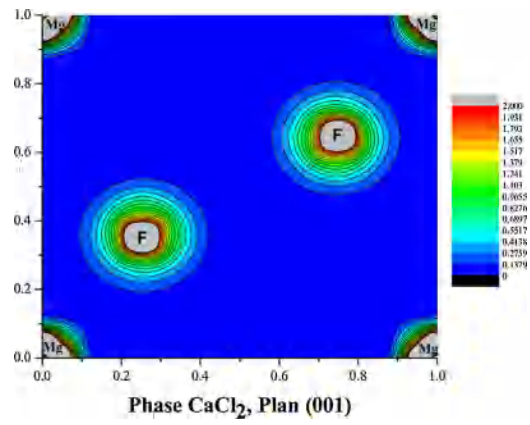**Fig. 16.** Arrangement of MgF$_2$ atoms in the rutile phase.

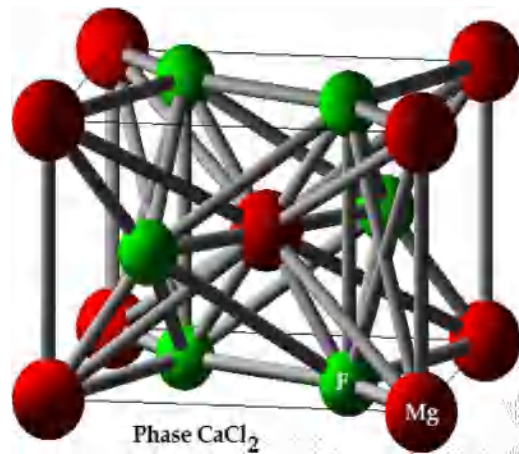**Fig. 17.** Charge density of the CaCl$_2$ phase of MgF$_2$ in the (001) plane.

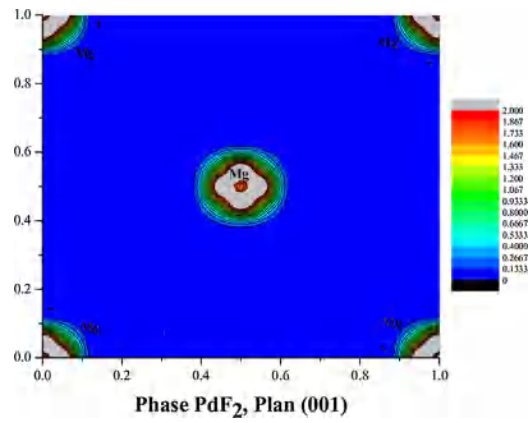**Fig. 18.** Arrangement of MgF$_2$ atoms in the CaCl$_2$ phase.
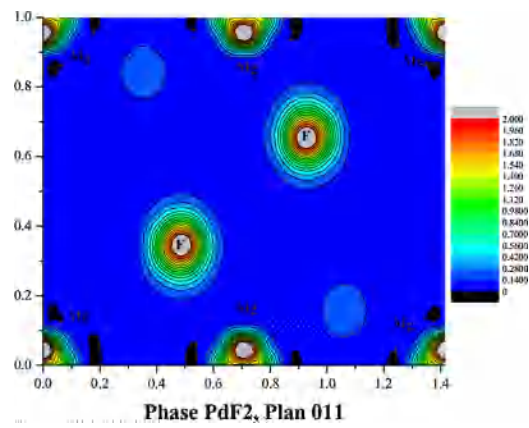
Fig. 19. Charge density of the PdF$_2$ phase of MgF$_2$.

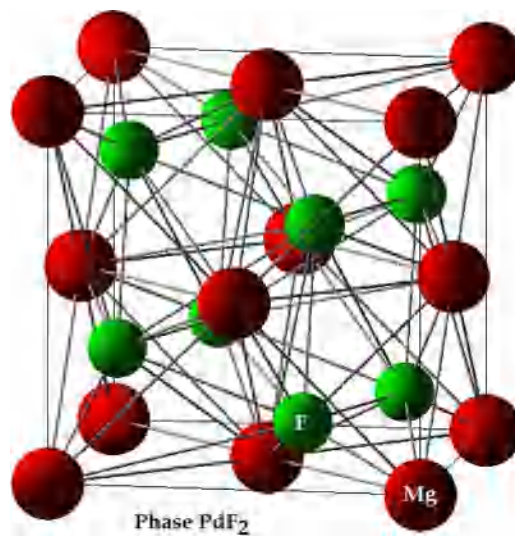**Fig. 20.** Charge density of the PdF$_2$ phase of MgF$_2$.

Fig. 21. Arrangement of MgF$_2$ atoms in the PdF$_2$ phase.

4. Conclusion

In this work, we calculated the structural, electronic and optical properties of MgF$_2$ in three phases in which our material is likely to crystallize. We also checked the phase transitions. The most remarkable is the similarity between the properties of the three phases at all levels (gaps, optical constants, ionicity). The comparison between our results and the literature showed a satisfactory agreement.

The electronic properties show a great resemblance between the values of the gaps, which proved to be direct in Γ for the three phases. These gaps are very wide, indeed the LDA gives ~7 eV, which is underestimated compared to the reality (due to a defect related to the method).

A result that seems very important to us is the non-participation of the d̈orbitals at the level of the states near the gap, which could explain (at least in part), the very large value of the gap.

References

[1] H.K. Pulker, Appl. Opt. 18 (1979) 1969.
[2] O. Duyar, H.Z. Durusoy, Turk. J. Phys. 28 (2004) 139.
[3] Y. Kitamura, N. Miyazaki, T. Mabuchi, T. Nawata, J. Cryst. Growth 311 (2009) 3954.
[4] F. Perales, D. Soto, Thin Solid Films 518 (2010) 4221.
[5] S. Chen, H. Shi, F. Cheng, C. Chen, W. Huang, Org. Electron. 13 (2012) 3263.
[6] B.E. Douglas, S. Ming Ho, Structure and Chemistry of Crystalline Solids, vol. 346, Springer Science + Business Media, Inc., Pittsburgh, PA, USA, 2006, pp. 64.
[7] P. Muller, Pure Appl. Chem. 6 (1994) 1077.
[8] J.R. Dilworth, W. Hussain, A.J. Hutson, C.J. Jones, F.S. Mcquillan, Inorg. Synth. 31 (1997) 257.
[9] http://www.almazoptics.com/MgF2.htm.
[10] E. Francisco, J.M. Recio, M.A. Blanco, A. Martín Pendás, A. Costales, J. Phys. Chem. A 102 (1998) 1595.
[11] R. David, Lide Handbook of Chemistry and Physics, vol. 87, CRC Press, Boca Raton, FL, 1998, pp. 4.
[12] P. Patnaik, Handbook of Inorganic Chemicals, McGraw-Hill, 2002.
[13] J. Aigueperse, P. Mollard, D. Devilliers, M. Chemla, R. Faron, R. Romano, J. Pierre Cuer, Ullmann's Encyclopedia of Industrial Chemistry, Wiley-VCH, Weinheim, 2005.
[14] K. Ramesh Babu, Ch. Bheema Lingam, S. Auluck, Surya P. Tewari, G. Vaitheeswaran, J. Solid State Chem. 184 (2011) 343.
[15] J. Haines, J.M. Leger, F. Gorelli, D.D. Klug, J.S. Tse, Z.Q. Li, Phys. Rev. B 64 (2001) 134110.
[16] W.H. Baur, Acta Cryst. B 32 (1976) 2200.
[17] V. Kanchana, G. Vaitheeswaran, M. Rajagopalan, J. Alloys Compd. 352 (2003) 60.
[18] http://sourceforge.net/projects/elk/files/elk-3.1.12.tgz/download.
[19] F.D. Murnaghan, Proc. Natl. Acad. Sci. U. S. A. 30 (1944) 5390.
[20] L. Zhang, Y. Wang, T. Cui, Y. Ma, G. Zou, Solid State Commun. 145 (2008) 283.
[21] H. Öztürk, C. Kürkçü, C. Kürkçü, J. Alloys Compd. 597 (2014) 155.
[22] A. Neelamraju, J. Bach, C. Schon, D. Fischer, M. Jansen, J. Chem. Phys. 137 (2012) 194319.
[23] T. Zhang, Y. Cheng, L.V. Zhen-Long, J. Guang-Fu, M. Gong, Int. J. Mod. Phys. B 28 (2014) 1450026.
[24] J.P. Perdew, Y. Wang, Phys. Rev. B 45 (1992) 13244.
[25] F.U. Abuova, E.A. Rotomin, V.M. Lisitsyn, A.T. Akilbekov, S. Piskunov, Nucl. Instrum. Methods B 326 (2014) 314.
[26] A.D. Becke, J. Chem. Phys. 98 (1993) 5648.
[27] P. Durand, G. Farge, M. Lambert, J. Phys. Chem. Solids 30 (1969) 1353.
[28] V.M. Lisitsyn, L.A. Lisitsyna, M.I. Kalinin, V.M. Reiterov, V.A. Fedotov, Opt. Spectrosc. 43 (1977) 912.
[29] S. Adachi, GaAs and Related Materials: Bulk Semiconducting and Superlattice Propertie, World Scientific Publishing Co. Pte. Ltd., Singapore, 1999.